Journal of Applied Polymer Science

Indentation Size Effect of Multiple Orders of Magnitude in Polydimethylsiloxane

Andrew J. Wrucke,[1] Chung-Souk Han,[2] Partha Majumdar[3]
[1]Department of Civil Engineering, University of Wyoming, Laramie, Wyoming 82071
[2]Department of Mechanical Engineering, University of Wyoming, Laramie, Wyoming 82071
[3]Center for Nanoscale Science and Engineering, North Dakota State University, Fargo, North Dakota 58105
Correspondence to: C.-S. Han (E-mail: chan1@uwyo.edu)

ABSTRACT: Indentation tests at indentation depths from 200 nm up to 100 μm were performed on polydimethylsiloxane (PDMS). The universal hardnesses in the elastomer were determined by microindentation and nanoindentation systems with Berkovich indenter tips and exhibited enormous increases of several orders of magnitude with decreasing indentation depth. Frank elasticity type molecular interactions were suggested as a rationale for the observed indentation size effect, which could have been related to material models with rotational gradients. A corresponding hardness model yielded good agreement with the experimental data. Other explanations for the indentation size effects in polymers in the literature are discussed in view of these experimentally determined and astonishing hardness increases in PDMS. © 2012 Wiley Periodicals, Inc. J. Appl. Polym. Sci. 000: 000–000, 2012

KEYWORDS: elastomers; mechanical properties; properties and characterization

Received 29 February 2012; accepted 6 June 2012; published online
DOI: 10.1002/app.38161

INTRODUCTION

There is mounting evidence that polymers exhibit size-dependent deformation. Size-dependent deformation has been observed in microbeam bending,[1,2] indentation tests,[3–10] composite materials,[11] and foams[12] at micrometer to submicrometer length scales. In contrast to metals, however, where size-dependent deformation at these length scales is commonly associated with geometrically necessary dislocations (see, e.g., Han et al.[13] and the references listed therein), the origin of size-dependent deformation in polymers is still not clear. In contrast to metals, the length-scale-dependent deformation seems also to vary strongly in magnitude and character with the polymer, as shown in Figure 1, where the hardness (H) over the indentation depth (h) of various polymers are shown. Therein, ultra-high-molecular-weight polyethylene (UHMWPE) and polytetrafluoroethylene (PTFE), for instance, do not exhibit an increase in H with deceasing h, whereas other polymers show different magnitudes of increases in the hardness. Among the polymers shown in Figure 1, the silicone rubber studied by Zhang and Xu[7] exhibited particularly remarkable behavior. Although at macroscopic length scales polydimethylsiloxane (PDMS) is a soft material that is actually softer than all the other polymers in Figure 1, at h's below 2 μm, its hardness increases strongly and exceeds other polymers below about $h = 300$ nm. Unfortunately, there was no detail in Zhang and Xu's article[7] on how the silicone sample was fabricated. Silicone rubber may contain fillers, and such filled silicone rubber also exhibits indentation size effects at h values above 1 μm.[9] To find some clarity on the origin of the size-dependent deformation of polymers in general and silicone rubber in particular, indentation tests on a chemically pure form of silicone rubber, namely, PDMS, were performed in this study over multiple length scales in h.

Probably one of the widest test ranges of h's were performed in this study. For a range from 100 μm down to about 200 nm in h, amazing indentation size effects were observed in PDMS, where the hardness increased multiple orders of magnitude. These results were analyzed and are discussed with respect to our earlier work and that of others in the literature.

EXPERIMENTAL

Material

The PDMS samples were fabricated from materials provided from Gelest (Morrisville, PA). The material consisted of a base of divinyl-terminated PDMS [molecular weight (MW) = 17,200 g/mol] and a curing/crosslinking agent, tetrakis(dimethylsiloxy)-silane (MW = 328.73 g/mol). The vinyl base and Karstedt's catalyst solution were combined in a 60-mL cup and mixed for 2 min at 1300 rpm with a DAC 150FVE-K speed mixer (FlackTek Inc., Landrum, SC). This solution was then placed in a vacuum oven for 15 min to remove air bubbles within the mix. The

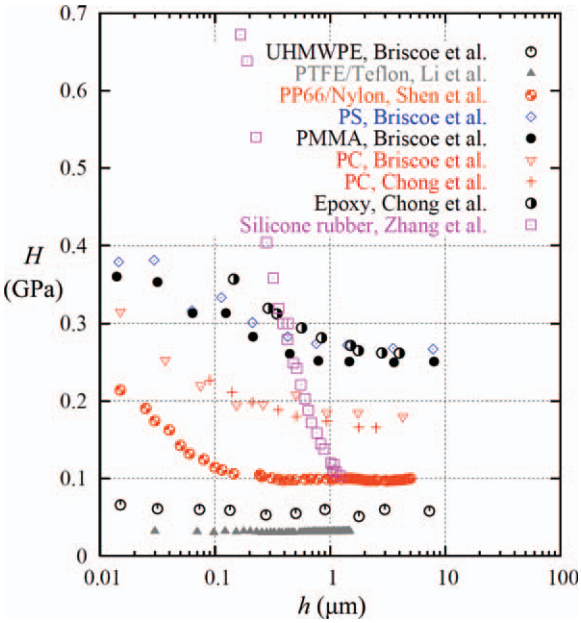

Figure 1. H versus h of various polymers. Data from Briscoe et al.[14] [UHMWPE, polystyrene (PS), poly(methyl methacrylate) (PMMA), and polycarbonate (PC)], Li and Bhushan[15] (PTFE), Chong and Lam[3] (PC and epoxy), Shen et al.[6] [polyamide 66 (PP66)], and Zhang and Xu[7] (silicone rubber). [Color figure can be viewed in the online issue, which is available at wileyonlinelibrary.com.]

curing/crosslinking agent was then added, and the entire compound was placed in the mixer for an additional 30 s. The entire solution was then deposited into polystyrene (PS) Petri dishes (47 or 35 mm in diameter, Fisher Scientific, Waltham, MA) to prevent deformation and damage to the material during handling. Finally, the PDMS solution was then cured at room temperature for 24 h and, then, additionally for a week at room temperature before testing. The samples were prepared with a crosslinker agent mass ratio ($M_{crosslinker}/M_{total}$, where $M_{crosslinker}$ is the mass of the crosslinker and M_{total} is the total mass of the mixture) of 0.6 g/40.0 g. The prepared samples were transparent and had smooth surfaces with no visible defects.

Indentation Testing

Indentation is a widely applied testing approach for polymers,[16–18] and both nanoindentation and microindentation tests have been conducted on PDMS samples. The nanoindentations were performed on MTS NanoXP indentation systems in the XP mode (MTS Systems, Eden Prairie, MN), whereas larger depths were tested with a Fischerscope HM2000S microindenter (MI; Fischer Technologies, Windsor, CT). Berkovich indenter tips were used in all of the tests. The nanoindentation tests were performed at different locations (University of Minnesota and University of Colorado at Boulder), and different Berkovich indenter tips were used.

All of the experiments were conducted with the application of a linear relationship between time and force at an ambient temperature of about 22°C. Force controlled loading was, therefore, applied, and corresponding displacements of the indenter tip were determined by the systems. The universal hardness (H_U) was evaluated from these data according to ISO 14577-1[19] at the maximal indentation force. As discussed in Tatiraju and Han,[9] the so-performed experiments with a conically shaped tip should have resulted in strain and strain rate fields that were affine to and on scale with the maximal h. Consequently, the hardness should not have changed with h, under the assumption that conventional local continuum mechanics were applicable. To validate the instrument, applied approach tests on a fused silica sample were conducted; these showed a less than 3% variation in the measured H_U, as shown in Figure 2, where a loading time of 5 s was applied.

RESULTS

As a rubber, PDMS deformed almost exclusively elastically in the indentation tests. In Figure 3(a), the typical loading–unloading data of the tests performed with the MI are shown, where the loading and unloading curves are almost identical so that more than 98% of the total indentation work was actually elastic. The indentation tests with the nanoindenter (NI) systems had similar characteristics, albeit the inelastic portion of the indentation work appeared to increase somewhat with decreasing h, as was also observed in Tatiraju and Han[9] for filled silicone rubber.

The indentation hardness (H_I)[20] as a measure of the resistance to permanent deformation and damage[19] is often evaluated to study the indentation size effect of a material. H_I is determined

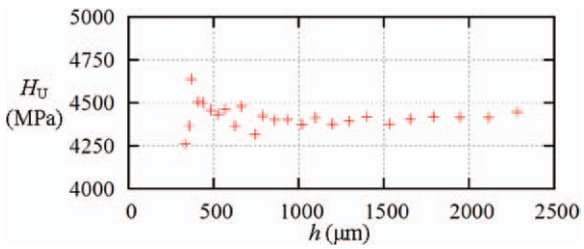

Figure 2. H_U versus h of fused silica with the NI. [Color figure can be viewed in the online issue, which is available at wileyonlinelibrary.com.]

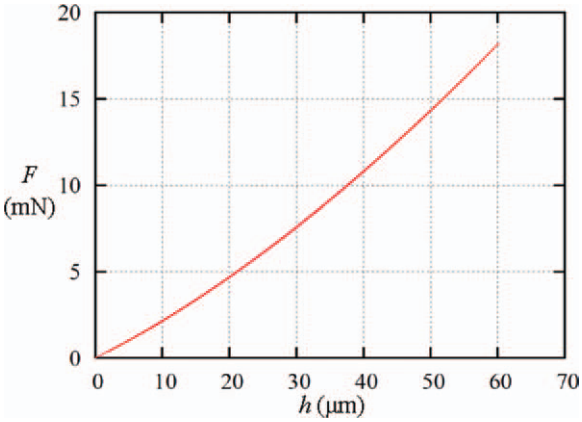

Figure 3. Sample microindentation loading and unloading curve of the PDMS sample at the 80-s loading time illustrating the highly elastic nature of the deformation. [Color figure can be viewed in the online issue, which is available at wileyonlinelibrary.com.]

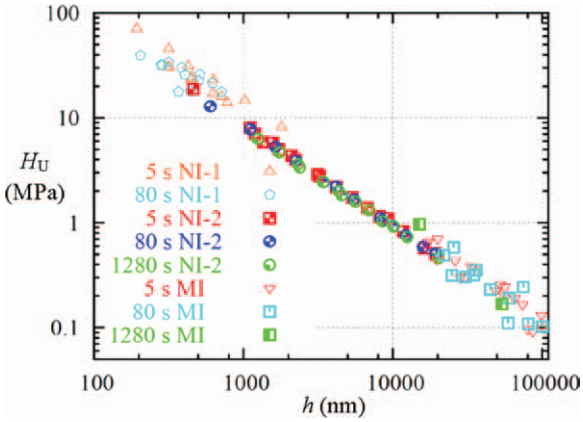

Figure 4. h versus H_U of PDMS of the different indentation systems. [Color figure can be viewed in the online issue, which is available at wileyonlinelibrary.com.]

by a projection technique that approximates the contact area at the maximal h of an indentation test. Here, we considered this approach to PDMS to not be reliable because, unlike in metals, the elastic deformation and strain was not small, and the projection[20] of the contact area for H_I did not result in valid data for the actual contact area.[21] Unlike H_I, H_U, also known as *Martens hardness*, can be applied to all materials[19] because a projection of the contact area is not needed, and the nominal contact area [$A_S(h)$; the surface area of the indenter penetrating beyond the zero point of contact, that is, the initial surface of the indented material] is applied for its evaluation. For the Berkovich indenter tip, this $A_S(h)$ is given as follows:

$$A_S(h) = 26.43\,h^2 \tag{1}$$

where h is the indentation depth under the applied test force. The H_U for each indentation test was calculated according to ISO 14557-1,[18] that is

$$H_U = \frac{F}{A_S(h)} \tag{2}$$

where F is the maximum applied force.

In Figure 4, the h versus H_U data for the PDMS is shown in logarithmic scale of the tests performed with the indenters. Herein, the data could be distinguished with respect to the three different instruments, that is, nanoindenter 1 (NI-1), nanoindenter 2 (NI-2), and MI. The indentation testing related to Figure 4 was conducted over a longer period of time. Although the testing with NI-2 was conducted within a week, the tests with NI-1 and the microindentations were performed over a period of several months. The aging or room-temperature curing of the samples could account for the scatter and corresponding higher hardnesses seen within these testing ranges. Particularly, the data obtained with the MI may have been the most significantly affected by additional curing, as the first tests were performed with the MI only about a week after the samples were fabricated. An increased hardness in tests conducted later was also observed by Deuschle et al.,[22] where details on the indenter tip were not provided. Also, in addition to the higher hardness of the indentations performed with NI-,1 there was also more scatter in these indentations. This may have been partly related to the different curvature radii (r's) of the indenter tips (discussed in more detail below) or to the surface roughness, which may have affected the indentation tests at smaller h's. Despite this scatter below 1000 nm, the general trend clearly showed that the hardness increased with decreasing h. It is worth noting that the hardnesses in Figure 4 were considerably lower than H_I of Zhang and Xu[7] on silicone rubber, as shown in Figure 1.

Although the determined hardness of h's above 6 μm should be unproblematic[19] for shallower depths, the hardness can be significantly affected by tip imperfections. To assess the influence of tip bluntness, the r's of the NI tips were determined with the approaches of Oliver and Pharr[20] and Troyon and Huang.[23] Hereto, the r values were obtained in several steps. First, the contact area function parameters[20] were obtained from the nanoindentation systems during calibration on fused silica. The projected contact area (A_C) as a function of h was used to fit the corresponding cone contact area function of Troyon and Huang;[23] this was determined with r for a cone angle that had the same area-to-depth ratio as the Berkovich tip. The so-determined r yielded 135 and 60 nm (rounded up to the next 5 nm), respectively, for the NI systems. r of the MI tip was warranted by the manufacturer to be less than 500 nm, and as the smallest h applied with the MI was well above 6 μm, the bluntness of the MI tip should have hardly affected the experimental results.

To assess the quality of the H_U data determined with the NIs, the error in A_S due to tip roundness was determined. For a perfect tip, the nominal surface area (A_S^{perfect}) is identical to eq. (1), that is

$$A_S^{\text{perfect}}(h) = 26.43\,h^2 \tag{3}$$

According to Troyon Huang,[23] the nominal surface area (A_S) of the Berkovich tip was compared with a conical tip. The nominal surface area for a cone with a rounded tip (A_S^{rounded}) can be determined as follows:

Applied Polymer SCIENCE

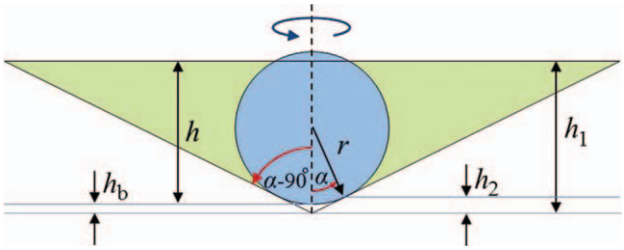

Figure 5. r and the lengths h_1, and h_2 for the determination of A_S^{rounded}. [Color figure can be viewed in the online issue, which is available at wileyonlinelibrary.com.]

$$A_S^{\text{rounded}} = 26.43(h_1^2 - h_2^2) + 2\pi r^2[1 - \cos(90^\circ - \alpha)]$$

where the parameters h_1, $h_2 = r \sin\alpha \tan\alpha$, and α [$= 19.55^\circ$ for a perfect cone eq. (3)] are defined in Figure 5.

For the rounded indenter tip, the difference in h with respect to a perfect indenter tip (please, see Figure 5) can be expressed with

$$h_b = r\left(\frac{1}{\sin(90^\circ - \alpha)} - 1\right) \tag{4}$$

Therefore, the actual h for a rounded tip is $h = h_1 - h_b$. In terms of h, the nominal surface area can be given with

$$A_S^{\text{rounded}} = 26.43(h + h_b)^2 - 26.43\, r^2\sin^2\alpha\, \tan^2\alpha + 2\pi r^2[1 - \cos(90^\circ - \alpha)] \tag{5}$$

Figure 6 illustrates the relative error (Δ_{rel})over h:

$$\Delta_{\text{rel}} = \frac{A_S^{\text{rounded}} - A_S^{\text{perfect}}}{A_S^{\text{perfect}}} \times 100 \tag{6}$$

For the applied range 200 nm $< h <$ 100 μm of h's, Δ_{rel} in A_S with respect to a perfect indenter tip should, therefore, be less than 10%. All of the H_U data presented here should, hence, have been quite unaffected by these r's besides data of h's below about 200–300 nm.

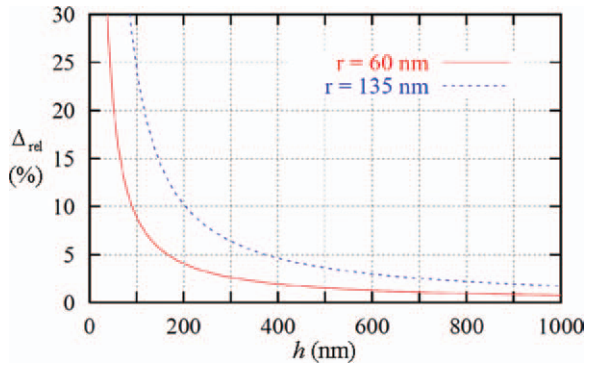

Figure 6. Δ_{rel} of nominal area in percentage between A_S^{perfect} and A_S^{rounded} with $r = 60$ nm and $r = 135$ nm versus h. [Color figure can be viewed in the online issue, which is available at wileyonlinelibrary.com.]

ANALYSIS OF THE EXPERIMENTAL DATA

The indentation size effects were rationalized here with molecular interactions of Frank energy[24] type, as suggested by Nikolov et al.[25] where the rotational gradients of the phenomenological couple stress theory of Yang et al.[26] were related to a Frank energy[24] type elastic potential. This theory was expanded to include plastic deformation, and a corresponding hardness model[27] has been suggested as follows:

$$H = H_0\left(1 + \frac{c_\ell}{h}\right) \tag{7}$$

where H_0 is the macroscopic hardness of the material and c_ℓ is the length scale parameter of the material. This hardness model has been successfully applied for other polymers[10] and filled silicone rubber,[9] albeit for smaller ranges of h than used in this study. For polymeric materials, c_ℓ can be related to the Frank energy parameter (K), that is, c_ℓ should be approximately proportional to K (see Han and Nikolov[27]). As K is known to depend on the bending rigidity, contour length, and MW of the polymer chain,[28] among other properties, this notion[27] would be able to explain the different length-scale-dependent behaviors of the polymers.[10]

To illustrate the linearity of the hardness to $1/h$, the abscissa is often chosen as such;[7] this is also shown in Figure 7, where the indentation data of Figure 4 is replotted with respect to $1/h$. Figure 7 is dominated by data below $h = 1$ μm and, therefore, by the data that had quite some scatter. In Figure 8, the $1/h$ versus H_U data is shown, with the experimental data below 1 μm h excluded. Although the differences in the data of loading times of 5 and 80 s was quite small and almost indistinguishable, there were some noticeable differences between 80 and 1280 s, although the differences were still rather small. In Figures 7 and 8, only one magnitude in h was adequately represented by the application of $1/h$ as the abscissa. Because multiple orders in h were considered here, the experimental data, along with their fits of the experimental data with eq. (7) is shown logarithmically in

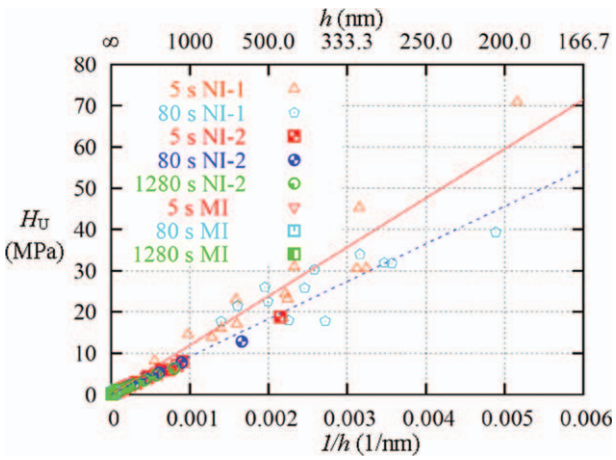

Figure 7. H_U versus $1/h$ for the whole range of data shown in Figure 2. [Color figure can be viewed in the online issue, which is available at wileyonlinelibrary.com.]

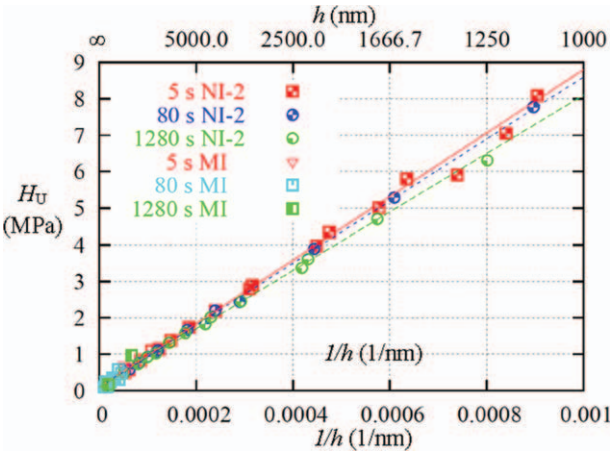

Figure 8. Comparison of the loading times and $1/h$ analysis (data of Figure 4 for $h = 1$–100 μm). The data here does not include the tests performed with NI-1. [Color figure can be viewed in the online issue, which is available at wileyonlinelibrary.com.]

Figure 9, which results in a relatively good agreement. Interestingly, Fakirov[29] also stated a linear relationship between H and $1/h$, that is, $H \approx 1/h$, without discussions and experimental data on this relation.

DISCUSSIONS

Besides the previously suggested rationale for the indentation size effects in PDMS, other explanations have been suggested in the literature, and these include (1) surface roughness, (2) adhesion, (3) friction, and (4) material inhomogeneity through the thickness. These rationale were previously discussed by Han.[10] In view of the data presented here, the wide range of h's, and the astonishing indentation size effects in PDMS, these explanations are reconsidered and discussed in the following.

Surface roughness

The roughness of the surfaces has been suggested as an explanation for indentation size effects.[7,30] In this respect, one should note that the surfaces of similarly fabricated PDMS samples showed low surface roughnesses of 20 nm[31] and less than 10 nm.[32] Although the surface roughness may be able to explain the indentation size effects at indentations depths below about 500 nm, the indentation size effects observed here appeared at indentation depths far higher than 500 nm. Therefore, the indentation size effect appeared at h, where any effects related to the surface roughness should not be relevant.

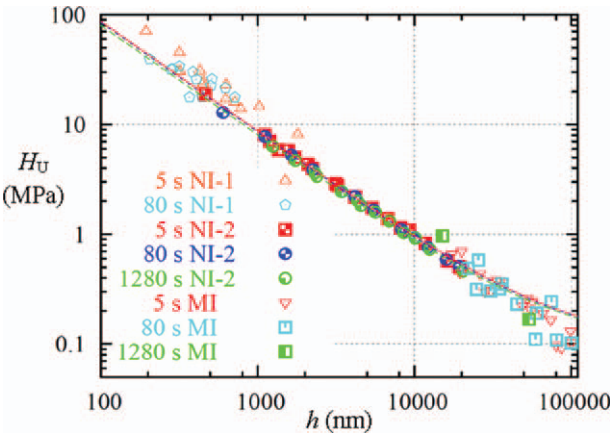

Figure 9. Data of Figure 4 with fitted curves of Figure 8. [Color figure can be viewed in the online issue, which is available at wileyonlinelibrary.com.]

Adhesion

In investigations where the adhesion was significantly affected, in the indentation experiments, the indenter tip was essentially spherical.[32,33] Here, a Berkovich indenter tip was used, and the tested material did not show the initial negative loading exhibited previously for adhesion.[31] Adhesion effects with a sharp conical tip are also only relevant at relatively small h's, well below 1 μm.[31] For these conducted experiments, the indentation size effects were present at higher h's and could not be explained by adhesion.

Friction

The applied indenter tip area was relatively flat, and the friction should, therefore, be small. Classical friction models, such as Coulomb friction, should scale with h and, therefore, not result in increased hardness, as finite element simulations of indentation experiments have shown.[34] An increase in the hardness due to friction would, consequently, require the friction coefficient to increase with the decreasing h. In view of the enormous increases in hardness, corresponding enormous increases in the friction coefficient would have to occur, which would be difficult to explain.

More importantly, friction is a highly dissipative process. The deformation in indentation testing, however, especially at higher h's, were almost exclusively elastic. Therefore, friction should only play only a minor role in the deformation process. Because of the enourmous increases in hardness with decreasing h, friction, therefore, appears unreasonable as an explanation.

Variation of the material properties through the depth from surface

In metals, the deformation mechanisms close to the surface can change significantly.[35] In polymers, too, changes in the material behavior, such as an increase in the viscosity, have been observed close to the vicinity of the surface.[36] These effects are, however, related to length scales below about 100 nm, and their influence should, therefore, not be significant for h's above 1 μm.

A change in the material properties due to the fabrication process, however, might be able to explain the changes in hardness with decreasing h. For instance, the crosslink denisty of the PDMS maybe have been higher at the surface than in the interior of the material; this resulted in a corresponding increase in the elasticity modulus. Although changing the processing method of the material samples did not affect the indentation size effects with spherical indenter tips at h's of up tp 300 nm,[37] the possibility of changing the material properties through the thickness is considered in the following text.

Although the approach of Oliver and Pharr[20] has been found not to be valid for PDMS,[21] it might serve at least as a rough approximation. According to Oliver and Pharr,[19] the elasticity modulus, E, can be calculated with:

$$\frac{1}{E_r} = \frac{1-\upsilon^2}{E} + \frac{1-\upsilon_i^2}{E_i} \tag{8}$$

where E_i and v_i are the elastic properties of the tip and E_r is the reduced modulus. E_r can be defined as follows:

$$E_r = d^* \frac{H_U}{1 - W_p/W_t} \tag{9}$$

where d^* is a constant equal to 4.678 for Berkovich indenter tips[38] and W_p and W_t are the plastic and total deformation work in the indentation process, respectively. For our PDMS material, the ratio W_p/W_t was quite small, as the deformation was highly elastic. Because E_i of the diamond tip was also very large compared to E of the PDMS samples, the terms W_p/W_t and $(1 - v^2)/E_i$ in eqs. (8) and (9) are neglected. Combining eqs. (8) and (9) yields

$$E = d^*(1-\upsilon^2)H_U \tag{10}$$

As E is, therefore, linearly proportional to H_U, increases of almost 3 orders of magnitude in E should be also present in the material. This evokes the question of what changes in the molecular structure may cause such an increase in the elasticity modulus. It is known that the crosslink density has a direct correlation to the elasticity modulus. Increases in the crosslinker in the fabrication process result in a saturation point, where additional increases in crosslinker do not result in higher crosslink densities.[39] The hardness and corresponding elasticity modulus based on eq. (10) at submicrometer h's would be very high to be achieved with increasing crosslinker. Also unclear is what mechanism could cause higher crosslink densities close to the surface. Changes in the crosslink density through the depth due to the fabrication process are, therefore, unlikely explanations for the strong increases in the hardness.

In this respect, it might also be worth noting that the samples were kept in the laboratory at a constant temperature. Changes in the humidity were not recorded, but the laboratory was not used for sample preparation or any other activities that would increase humidity other than present personnel. Significant effects related to humidity were, therefore, not able to explain the observed effects because the indentation size effect was observed for whole range of h's of up to 100 μm. With regard to aging, we recently performed some indentation tests at small h's on Sylgard PDMS samples fabricated as in Lim and Chaudhri,[21] where the tests were conducted a day after fabrication. The hardness at small h in these tests was also highly elevated, similar to those reported in this article. We, therefore, concluded that although aging might have had a certain influence on the hardness, it was not be able to explain the hardness increases of several orders of magnitude. Likewise surface detection might pose a problem at lower indentation depths but would not be able to explain the depth dependent universal hardness at larger indentation depths.

CONCLUSIONS

Indentation test at h's from 200 nm up to 100,000 nm were performed. The experimentally determined H_U's showed enormous increases of several orders of magnitude with decreasing h. For the increase in hardness, an earlier suggested constitutive theory rotational gradient incorporating a Frank energy type potential and a corresponding hardness model were considered. The constitutive theory can relate molecular interactions to rotational gradients. The hardness model corresponding to the constitutive rotational gradient theory that was developed in an earlier article resulted in good fits with the experimental data. Other explanations for the indentation size effects in the polymers were discussed in view of the observed amazing indentation size effects in PDMS.

ACKNOWLEDGMENTS

Indentation tests were carried out at the Characterization Facility, University of Minnesota, part of National Science Foundation funded Materials Research Facilities Network (http://www.mrfn.org), and at the Nano Characterization Facility, University of Colorado at Boulder. The use of the MI of the Department of Civil Engineering at the North Dakota State University was also appreciated. The authors also thank Elizabeth Crowley at Center for Nanoscale Science and Engineering (CNSE) for the fabrication of the samples. This work was supported by CAREER Award of the National Science Foundation under contract grant number CMMI-0846692/1102764.

REFERENCES

1. Lam, D. C. C.; Yang, F.; Chong, A. C. M.; Wang, J.; Tong, P. *J. Mech. Phys. Sol.* **2003,** *51*, 1477.
2. McFarland, A. W.; Poggi, M. A.; Bottomley, L. A.; Colton, J. S. *Nanotechnology* **2004,** *15*, 1628.
3. Chong, A. C. M.; Lam, D. C. C. *J. Mater. Res.* **1999,** *14*, 4103.
4. Lam, D. C. C.; Chong, A. C. M. *J. Mater. Res.* **1999,** *14*, 3784.
5. Lam, D. C. C.; Chong, A. C. M. *Mater. Sci. Eng. A* **2000,** *281*, 156.
6. Shen, L.; Phang, I. Y.; Liu, T.; Zeng, K. *Polymer* **2004,** *45*, 8221.
7. Zhang, T.-Y.; Xu, W.-H. *J. Mater. Res.* **2002,** *17*, 1715.
8. Tjernlund, J. A.; Gamstedt, E. K.; Xu, Z. H. *Polym. Eng. Sci.* **2004,** *44*, 1987.
9. Tatiraju, R. V. S.; Han, C.-S. *J. Mech. Mater. Struct.* **2010,** *5*, 277.
10. Han, C.-S. *Mater. Sci. Eng. A* **2010,** *527*, 619.
11. Tjernlund, J. A.; Gamstedt, E. K.; Gudmundson, P. *Int. J. Sol. Struct.* **2006,** *43*, 7337.
12. Lakes, R. S. *Int. J. Sol. Struct.* **1986,** *22*, 55.
13. Han, C.-S.; Ma, A.; Roters, F.; Raabe, D. *Int. J. Plast.* **2007,** *23*, 690.
14. Briscoe, B. J.; Fiori, L.; Pelillo, E. *J. Phys. D* **1998,** *31*, 2395.
15. Li, X.; Bhushan, B. *Thin Solid Films* **2000,** *377–378*, 401.

16. Konnerth, J.; Stockel, F.; Muller, U.; Gindl, W. *J. Appl. Polym. Sci.* **2010,** *118*, 1331.
17. Bauer, M.; Hartmann, L.; Kuschel, F.; Seiler, B.; Noack, E. *J. Appl. Polym. Sci.* **2010,** *117*, 1924.
18. Tang, X.-G.; Hou, M.; Truss, R.; Zou, J.; Yang, W.; Dong, Z. G.; Huang, H. *J. Appl. Polym. Sci.* **2011,** *122*, 885.
19. ISO 14577–1; Metallic Materials—Instrumented Indentation Test for Hardness and Materials Parameters—Part 1: Test Method; International Organization for Standardization: **2002.**
20. Oliver, W. C.; Pharr, G. M. *J. Mater. Res.* **1992,** *7*, 1564.
21. Lim, Y. Y.; Chaudhri, M. M. *Mech. Mater.* **2006,** *38*, 1213.
22. Deuschle, J. K.; de Souza, E. J.; Arzt, E.; Enders, S. *Int. J. Mater. Res.* **2010,** *101*, 1014.
23. Troyon, M.; Huang, L. *J. Mater. Res.* **2005,** *20*, 610.
24. de Gennes, P. G.; Prost, J. The Physics of Liquid Crystals; Oxford University Press: **1993.**
25. Nikolov, S.; Han, C.-S.; Raabe, D. *Int. J. Sol. Struct.* **2007,** *44*, 1582; Corrigendum. *Int. J. Sol. Struct.* **2007,** *44*, 7713.
26. Yang, F.; Chong, A. C. M.; Lam, D. C. C.; Tong, P. *Int. J. Sol. Struct.* **2002,** *39*, 2731.
27. Han, C.-S.; Nikolov, S. *J. Mater. Res.* **2007,** *22*, 1662.
28. Jamieson, A. M.; Gu, D. F.; Chen, F. L.; Smith, S. *Prog. Polym. Sci.* **1996,** *21*, 981.
29. Fakirov, S. *J. Mater. Sci.* **2007,** *42*, 1131.
30. Zhang, T.-Y.; Xu, W.-H.; Zhao, M.-H. *Acta. Mater.* **2004,** *52*, 57.
31. Charitidis, C. *Ind. Eng. Chem. Res.* **2011,** *50*, 565.
32. Carrillo, F.; Gupta, S.; Balooch, M.; Marshall, S. J.; Marshall, G. W.; Pruitt, L.; Puttlitz, C. M. *J. Mater. Res.* **2005,** *20*, 2820.
33. Liao, Q.; Huang, J.; Zhu, T.; Xiong, C.; Fang, J. *Mech. Mater.* **2010,** *42*, 1043.
34. Mata, M.; Alcala, J. *J. Mech. Phys. Solids* **2004,** *52*, 145.
35. Han, C.-S.; Hartmaier, A.; Gao, H.; Huang, Y. *Mater. Sci. Eng. A* **2006,** *415*, 225.
36. de Gennes, P. G. *Eur. Phys. J. E* **2000,** *2*, 201.
37. Tweedie, C. A.; Constantinides, G.; Lehman, K. E.; Brill, D. J.; Blackman, G. S.; Van Vliet, K. J. *Adv. Mater.* **2007,** *19*, 2540.
38. Constantinides, G.; Ulm, F. J.; Van Vliet, K. *Mater. Struct.* **2003,** *36*, 191.
39. Arima, T.; Hamida, T.; McCabe, J. F. *J. Dent. Res.* **1995,** *74*, 1597.